Controlled Introduction of sp^3 quantum defects in Fluorescent Carbon Nanotubes by Mechanochemistry

Miriam Sander+[a], Justus T. Metternich+[a,b], Pascal Dippner[a], Sebastian Kruss*[a,b], and Lars Borchardt*[a]

[a]   M. Sander[+], P. Dippner, Prof. Dr. L. Borchardt
       Department of Chemistry
       Ruhr-University Bochum
       Universitätsstraße 150, 44801 Bochum
       E-mail: lars.borchardt@rub.de

[b]   Dr. J.T. Metternich[+], Prof. Dr. S. Kruss
       Biomedical Nanosensors
       Fraunhofer Institute for Microelectronic Circuits and Systems (IMS)
       Finkenstraße 61, 47057 Duisburg
       E-mail: sebastian.kruss@rub.de

[+]   These authors contributed equally to this work.

       Supporting information for this article is given via a link at the end of the document.

Abstract: Precise control over low-dimensional materials holds an immense potential for their applications in sensing, imaging and information processing. The controlled introduction of sp^3 quantum defects (color centers) can be used to tailor the optoelectronic properties of single-walled carbon nanotubes (SWCNTs) in the tissue transparency (> 800 nm) and the telecommunication window. However, an uncontrolled functionalization of SWCNTs with defects leads to a loss of the NIR fluorescence. Here, we use mechanochemistry with aryldiazonium salts to create quantum defects in SWCNTs. The reaction proceeds within 5 min without solvents or illumination and can be controlled by a varied mechanochemical energy impact. By working in the solid-state, this method presents an alternative synthetic route and marks a crucial step for tailoring photophysics of SWCNTs.

Introduction

Carbon nanomaterials are promising solid-state materials for a wide range of applications.[1] Their optoelectronic properties depend on their structure and its controlled modification can be used to tailor their properties. Within the family of carbon nanomaterials, single-walled carbon nanotubes (SWCNTs) are especially interesting, as they possess an intrinsic fluorescence in the near-infrared (NIR) range of the spectrum.[2] The fluorescence of SWCNTs is depending on its chirality, which describes the structure of a SWCNT and can therefore be correlated to its band gap.[2] SWCNTs are photostable and their fluorescence is sensitive to the chemical environment.[3] This renders SWCNTs suitable for basic research and applications in molecular imaging[4], sensing[5] and light harvesting[6]. To tailor the optoelectronic properties to these applications different structural modifications have been developed.[7,8,9] One prominent example is the functionalization with sp^3 quantum defects, also known as (organic) color centers (OCCs), which leads to color center nanotubes (CCNTs).[10,11] Controlled introduction of such defects in the sp^2 lattice results in novel electronic states that cause an additional redshifted fluorescent feature (E_{11}*).[10,12,13,14] When introduced as single defects (around 5–10 defects per micrometer), the overall fluorescence can be increased.[12,13] However, an excessive functionalization of the lattice leads to a loss of the SWCNT fluorescence, as the (electronic) structure of the SWCNT is disrupted.[8,15] Depending on the SWCNT sample (aqueous or organic solvent, freestanding or deposited), different synthetic routes exist to achieve luminescent defects.[9,16] For applications in biosensing, methods that are compatible with aqueous environments are especially interesting but require a suitable surface coating to solubilize the highly hydrophobic SWCNTs. Most often, quantum defects are introduced via aryldiazonium salts, or the nucleophilic addition with 2-haloanilines in the presence of strong organic bases. Due to the ease of control as well as its favorable reaction kinetics, the synthetic approach with aryldiazonium salts is currently in the focus.[8]

To further advance the field, new larger-scale synthetic methods without the need of surfactant coating are desired. Here, the combination of fields that are typically not associated with each other promises new opportunities. Mechanochemistry is a sustainable branch of chemistry, in which ball mills are used to induce and sustain chemical reactions by mechanical energy.[17] In these solid-state reactions, the addition of solvents becomes obsolete. This allows, among others, to overcome limitations of solubility and to connect short reaction times with simple reactions' scale up.[18,19] So far, mechanochemical approaches have been successfully applied for the functionalization of varying carbonaceous materials such as CNTs[20], (activated) carbons[21] or graphite/graphene[22]. For CNTs' modification, its main application has been the reduction of the nanotube length.[23] Additionally, certain functional groups were introduced, however, these were not aimed at tailoring the SWCNT fluorescence.[24] To the best of our knowledge, there exists no study that demonstrates the mechanochemical introduction of sp^3 quantum defects with the level of control (1−10 defects in 100 000 carbon

atoms)[12] that is paramount to maintain the fluorescence of the SWCNT.

Here, we present the first mechanochemical approach to introduce sp^3 quantum defects in fluorescent SWCNTs under solid-state conditions. We show how different *i)* milling times, *ii)* ball sizes, and *iii)* the addition of water affects the functionalization and its controllability. To confirm the influence of the energy impact, we applied *iv)* resonant acoustic mixing as an alternative mechanochemical treatment.

Results and Discussion

To introduce sp^3 quantum defects mechanochemically, we treated (6,5)-chirality enriched CoMoCAT-SWCNTs (0.5 mg, 4.73 x10^{-7} mmol) with aryldiazonium tetrafluoroborate salts (R: NO$_2$ with 1.12 mg, 4.73 x10^{-3} mmol; R: OMe with 1.05 mg, 4.73 x10^{-3} mmol) in a MM400 mixer mill at 30 Hz (**Figure 1**a). For our first experiments, a milling vessel with a volume of 14 mL and milling balls made of polymers were applied. To guarantee a sufficient vessel filling and ball-to-powder ratio[25], sodium chloride was used as bulk material. To be able to analyze the defect density on the CCNTs, we studied both, the NIR fluorescence and the Raman spectra (**Figure 1**b). On the one hand, a controlled introduction of quantum defects leads to the new fluorescence feature E$_{11}$* as well as an increased D-mode in Raman spectra.[13] On the other hand, the D-mode further increases with an uncontrolled introduction of defects, and both fluorescence features E$_{11}$/E$_{11}$* are quenched and would ultimately disappear.

We first investigated the influence of the mechanochemical energy impact on the functionalization by varying the milling time (**Figure 2**). After 5 min of milling, we observed an increase of defect associated E$_{11}$* emission feature (**Figure 2**b, Figure S2) as well as defect associated D-mode in the Raman spectrum (Figure S14). The excitation-emission spectrum (**Figure 2**c) allowed the correlation between the new emission features and the respective E$_{11}$ feature of the (6,5)- and (6,4)-chirality (Figure S5). A prolonged milling (60 min) introduced a higher defect density (5 min: D/G = 0.078, 60 min: D/G = 0.172) but quenched the SWCNT fluorescence (**Figure 2**b). To quantify the mechanochemical impact, we subsequently compared the functionalization to a non-milled reaction approach, in which all
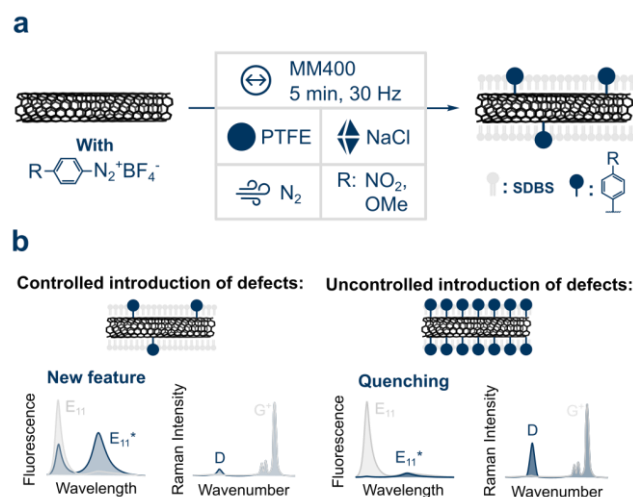

Figure 1. Mechanochemical functionalization of single-walled carbon nanotubes with sp^3 quantum defects. a) Reaction scheme with standard milling parameters: Treating SWCNTs with aryldiazonium tetrafluoroborate salts inside a MM400 mixer mill at 30 Hz. Using perfluoroalkoxy alkanes (PFA) milling vessel, polytetrafluoroethylene (PTFE) milling balls, NaCl as bulk material, nitrogen atmosphere and excluding illumination. Sodium dodecylbenzenesulfonate (SDBS) solution is only used for the work-up to perform fluorescence spectroscopy. b) Presentation of the controlled and uncontrolled introduction of quantum defects as well as their change in fluorescence and Raman spectra (grey: pristine SWCNT, blue: CCNTs).

reactants were simply mixed by hand. Because the reaction proceeds fast in aqueous environment during the work-up, the non-milled reaction showed a slightly increased E$_{11}$* emission (**Figure 2**b) compared to the pristine reference (Figure S2). Nevertheless, it was apparent that the defect density is increased due to the mechanochemical impact.

To examine whether sufficient mixing or the energy impact leads to the introduction of quantum defects, the diameter of milling balls (10 mm, 5 mm, 3 mm), the number of balls (#34, #5, #1), and the vessel volumes (V1: 14 mL, V2: 2 mL) were varied in the following (**Figure 3**). For comparison, the size and number of balls were normalized to the mass of balls meaning that only the surface area of balls changes. In general, a smaller ball size leads to better mixing, whereas a bigger ball size inserts higher energy during milling.[25,26] For all used ball sizes, the introduction of quantum defects was successful as the E$_{11}$* fluorescence increased during the mechanochemical reaction (**Figure 3**b).
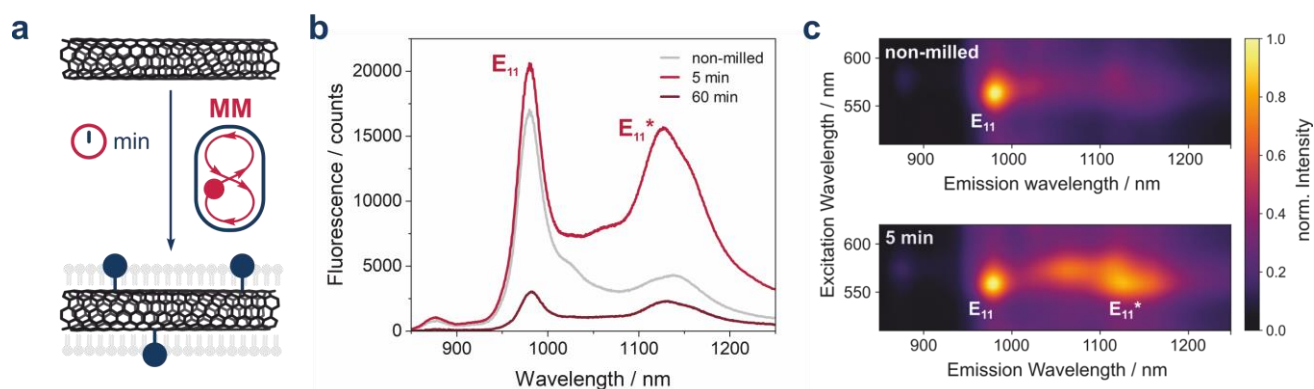

Figure 2. Influence of varying milling times on the mechanochemical introduction of sp^3 quantum defects in SWCNTs. a) Representation of the different milling conditions. SWCNTs were treated with 4-nitrobenzenediazonium tetrafluoroborate and NaCl as bulk material inside a mixer mill at 30 Hz. Milling was conducted by using varying milling times (5 min, 60 min), a 14 mL PFA milling vessel and one 10 mm-diameter PTFE milling ball. b) Fluorescence spectra of CCNTs after different milling times. c) Excitation-emission spectrum of the non-milled reaction mixture as well as after 5 min of milling.
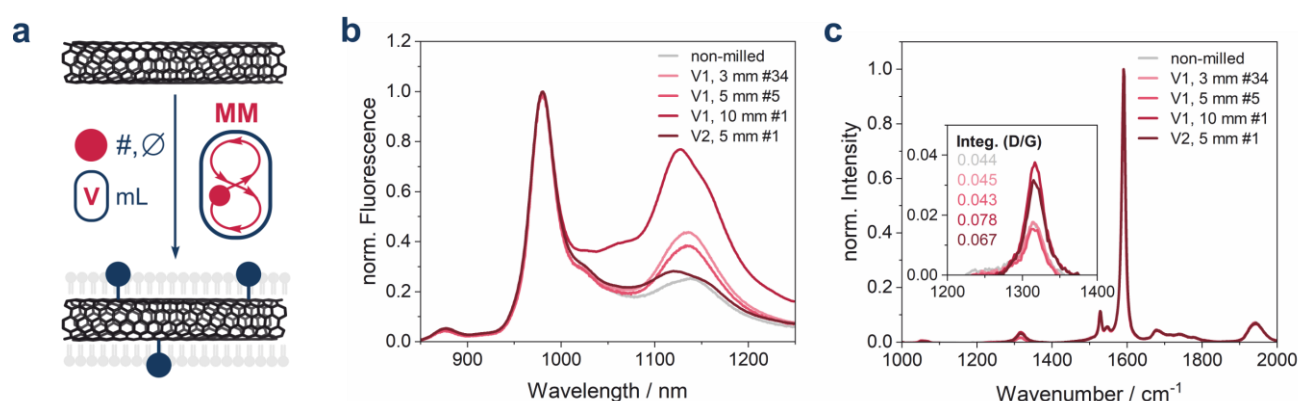
2

Figure 3. Influence of varying milling ball diameters, number of balls and vessel volumes on the mechanochemical introduction of sp^3 quantum defects in SWCNTs. a) Representation of the different milling conditions. SWCNTs were treated with 4-nitrobenzenediazonium tetrafluoroborate and NaCl as bulk material inside a mixer mill at 30 Hz for 5 min. Milling was conducted by using PTFE milling balls with varying diameter (10 mm, 5 mm, 3 mm) and number (#34, #5, #1), PFA milling vessels with varying volume (V1: 14 mL, V2: 2 mL) as well as NaCl as bulk material (2 g for V1, 0.2 g for V2). b) Normalized fluorescence spectra of CCNTs after different milling conditions. c) Raman spectra of CCNTs after different milling conditions as well as the ratios calculated from the integral of the D- to G-Raman mode.

Using one 10 mm-diameter ball, it was possible to sufficiently initiate and control the reaction, resulting in the highest $E_{11}*/E_{11}$ ratio. Interestingly, the varying mechanochemical energy impacts caused different results. While smaller ball diameters introduce single quantum defects, the higher energy impact of the ball likely reaches higher defect densities. Calculating the impact energy[27] of the collision between one ball with varying diameter and the reactants suggests as well that the energy must be sufficiently high (E_{impact} for 10 mm-diameter ball = 110 J) to increase the defect density (see Supporting information 3.3.). In accordance with the fluorescence spectra, we observed an increase of the D-mode in Raman spectra (**Figure 3**c) for the 10 mm-diameter ball (D/G = 0.078) compared to the non-milled control, but no significant change using the 3 mm- and 5 mm-diameter balls (see Supporting information 3.3.). To investigate how the bulk material affects the energy impact, we repeated the reaction in a 2 mL milling vessel with one 5 mm-diameter milling ball and reduced amount of NaCl (0.2 g). In contrast to the 10 mm-diameter ball in 14 mL vessel, the treatment in 2 mL vessel led to a comparatively high D/G ratio (**Figure 3**c) in combination with a low defect-related fluorescence (**Figure 3**b). It suggests structural disruption of the SWCNT due to too many defects. Another explanation might be the incorporation of non-fluorescent structural defects in the SWCNTs due to a high energy impact. The varied vessel volumes may cause different milling ball movements and thus different mechanical stress (impact vs. friction).[27,28] Based on the improved control over the defect density, we selected the one 10 mm-diameter ball in 14 mL milling vessel for the following experiments.

By changing the rheology of the reaction mixture, one can facilitate a neat mechanochemical reaction further. Commonly, it is enabled by simply adding a small volume of solvents into the milling vessel.[29,30] As fluorescent SWCNTs can be used in aqueous environments, we subsequently repeated the reaction with a small volume of water (200 μL, η = 0.1 μL mg^{-1} based on mass of solids, **Figure 4**). Compared to the neatly milled reaction (5 min), the SWCNT fluorescence was quenched after both 5 min and 60 min of milling with water (**Figure 4**b). In accordance, the D-mode in Raman spectra increased tremendously for the functionalization with added water leading to higher D/G ratios

(**Figure 4**d), which corresponds to a high defect density. While this degree of functionalization might be useful for the use in mechanical or electrical applications, it destroys the SWCNTs' fluorescence and therefore precise control of defect numbers is crucial.

To assess which functionalization introduces the defects, various control reactions were performed (**Figure 4**c). After milling SWCNTs and NaCl under nitrogen atmosphere (Figure S6 and S7), neither the fluorescence nor the Raman spectra indicated a
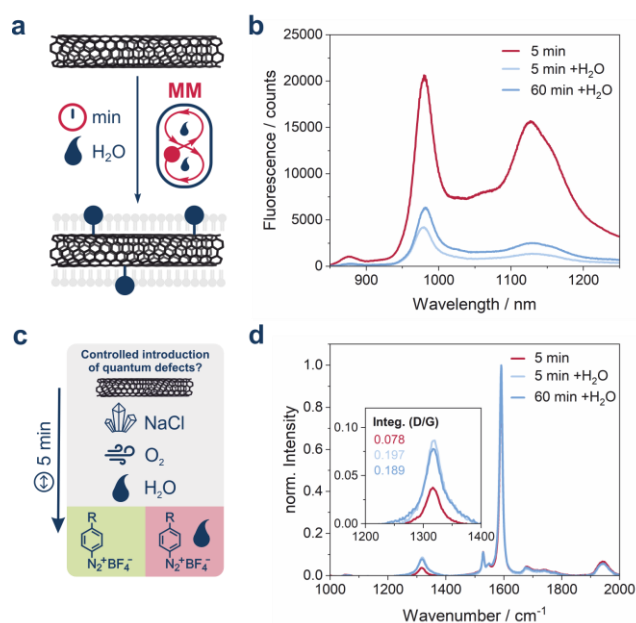

Figure 4: Addition of water for the mechanochemical introduction of sp^3 quantum defects in SWCNTs. a) Representation of the different milling conditions. SWCNTs were treated with 4-nitrobenzenediazonium tetrafluoroborate and NaCl as bulk material inside a mixer mill at 30 Hz. Milling was conducted by using water (V = 200 μL) as additive, varying milling times (5 min, 60 min), a 14 mL PFA milling vessel and one 10 mm-diameter PTFE milling ball. b) Fluorescence spectra of CCNTs after different milling conditions compared to the neat milling (5 min). c) Overview of possible reactants for the mechanochemical functionalization of SWCNTs and their influence on the controlled introduction of quantum defects (grey: no introduction of defects, green: controlled introduction of defects, red: uncontrolled introduction of defects). d) Raman spectra of CCNTs after different milling conditions as well as the ratios calculated from the integral of the D- to G-Raman mode.
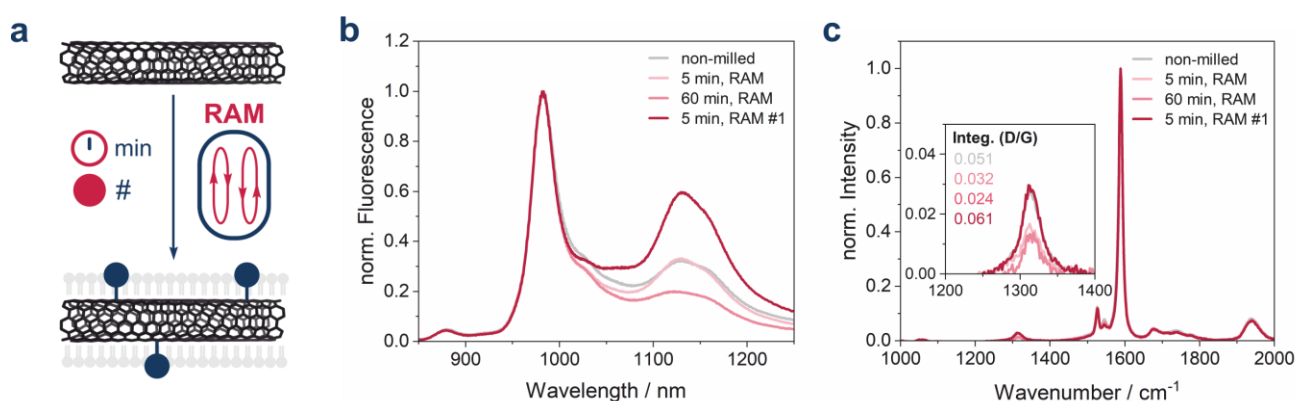
3

Figure 5. Application of resonant acoustic mixing (RAM) and varying mixing conditions for the mechanochemical introduction of sp^3 quantum defects in SWCNTs. a) Representation of the different milling conditions. SWCNTs were treated with 4-nitrobenzenediazonium tetrafluoroborate and NaCl as bulk material inside a LabRAM at 90 g. Milling was conducted by using a 14 mL PFA milling vessel, varying mixing time (5 min, 60 min) and varying number of 10 mm-diameter PTFE milling ball (none, one #1). b) Normalized fluorescence spectra of CCNTs after different milling conditions. c) Raman spectra of CCNTs after different milling conditions as well as the ratios calculated from the integral of the D- to G-Raman mode.

mechanochemical introduction of (sp^3 quantum) defects. Importantly, it verifies that the simple milling of SWCNTs does not lead to a change of their fluorescence properties. Additionally, we wanted to exclude the influence of oxygen and water. Therefore, we i) switched to ambient atmosphere to examine the influence of oxygen (Figure S6 and S7) and ii) added water as additive (Figure S6 and S7). For both reactions, neither the fluorescence nor the Raman spectra showed a significant difference to the spectra of pristine SWCNTs (Figure S2 and S3). We therefore conclude that the introduction of quantum defects is based on the mechanochemical reaction of SWCNTs with the aryldiazonium tetrafluoroborate salt. The non-milled control with added water (Figure S22) clarified that the functionalization starts without the mechanochemical impact, which is likely due to the highly concentrated diazonium salt concentration. Milling the reaction mixture for an additional 5 min or 60 min with added water led to a further, uncontrollable increase of the quantum defect density. It can be useful for other applications but again led to the unintended quenching of SWCNT fluorescence. To conclude, for the mechanochemical controlled introduction of quantum defects it is crucial i) to stay under solid-state, water-free conditions and ii) to adjust the energy impact, which perfectly plays out the advantages of mechanochemistry.

Notably, the chosen reactant 4-nitrobenzenediazonium tetrafluoroborate proved to be especially suitable for the mechanochemical quantum defect introduction. In contrast, 4-methoxybenzenediazonium tetrafluoroborate as an alternative reactant led to an uncontrolled introduction of defects due to its different reactivity (see Supporting information 3.5.). These results show that the reactivity of the compounds plays an important role. To assess qualitative changes of the SWCNT length by milling, we characterized our samples with dynamic light scattering (DLS, Figure S37). Overall, using different milling times as well as water as additive reduced the length by about half.

To demonstrate the importance of the mechanical impact during the introduction of quantum defects, we applied resonant acoustic mixing (RAM) as another reactor concept. Intended was not the further reaction development, but rather an additional control reaction. In contrast to conventional ball milling, RAM is carried out milling media-free and facilitates the mixing in the reaction mixture via fast movements. Thus, mechanical stress and localized high energy inputs by milling balls are avoided (**Figure 5**).[19,30,31] Applying the mixing time of 5 min and 60 min at 90 g, the E_{11}^* fluorescence and the D/G ratio did not increase compared to the non-milled control (**Figure 5**b, c). Here, the energy input might not be sufficient to overcome the activation barrier needed for the reaction of both reactants. Additionally, the diazonium salt might decompose with prolonged mixing. Importantly, this control reaction demonstrates the critical mechanical impact of the milling balls to initiate and to continue the mechanochemical functionalization. For further verification on this hypothesis, we added one 10 mm-diameter ball to the milling vessel in the RAM (**Figure 5**b, c). Here, we successfully introduced quantum defects within 5 min via mechanical impact.

Conclusion

In summary, we developed a straightforward mechanochemical method for the controlled introduction of sp^3 quantum defects in fluorescent SWCNTs by treatment with aryldiazonium tetrafluoroborate salts. Importantly, this method allows to create sp^3 quantum defects at the extremely low defect densities and chemical control required to serve as exciton traps without diminishing the intrinsic fluorescence of the SWCNTs. By variation of milling conditions, we identified the mechanical impact via milling balls as crucial to initiate the functionalization with sp^3 quantum defects and to control the reaction. The functionalization proceeds within 5 min in a mixer mill and the defect density can be further adjusted by varying the balls' surface area. In our study, a prolonged milling time led to a loss in fluorescence, whereas milling media-free techniques provided an insufficient energy impact to start the functionalization. As a result, the solid-state reaction conditions during the mechanochemical reaction proved to be decisive for the controlled introduction of defects and, in addition, benefits its feasibility of larger scale ups, as concentration dependent inhomogeneities during the conventional, light activation of the reaction may be overcome. Overall, we provide groundwork for mechanochemical reactions as a promising alternative for the functionalization of fluorescent

SWCNTs with sp^3 quantum defects. These materials promise applications from biosensing to photonics and NIR single photon sources for quantum computing.

Supporting Information

The authors have cited additional references within the Supporting Information.[32]

Acknowledgements

References

[1] a) G. Hong, S. Diao, A. L. Antaris, H. Dai, *Chem. Rev.* **2015**, *115*, 10816; b) R. Martel, T. Schmidt, H. R. Shea, T. Hertel, P. Avouris, *Appl. Phys. Lett.* **1998**, *73*, 2447.

[2] M. J. O'Connell, S. M. Bachilo, C. B. Huffman, V. C. Moore, M. S. Strano, E. H. Haroz, K. L. Rialon, P. J. Boul, W. H. Noon, C. Kittrell et al., *Science* **2002**, *297*, 593.

[3] a) J. G. Duque, M. Pasquali, L. Cognet, B. Lounis, *ACS nano* **2009**, *3*, 2153; b) M. Erkens, W. Wenseleers, M. Á. López Carrillo, B. Botka, Z. Zahiri, J. G. Duque, S. Cambré, *ACS nano* **2024**, *18*, 14532.

[4] a) A. Nadeem, S. Lyons, A. Kindopp, A. Jamieson, D. Roxbury, *ACS nano* **2024**, *18*, 22874; b) S. Kruss, D. P. Salem, L. Vuković, B. Lima, E. Vander Ende, E. S. Boyden, M. S. Strano, *Proc. Natl. Acad. Sci. U.S.A.* **2017**, *114*, 1789; c) L. Sistemich, P. Galonska, J. Stegemann, J. Ackermann, S. Kruss, *Angew. Chem. Int. Ed.* **2023**, *62*, e202300682; d) J. Ackermann, J. Stegemann, T. Smola, E. Reger, S. Jung, A. Schmitz, S. Herbertz, L. Erpenbeck, K. Seidl, S. Kruss, *Small* **2023**, *19*, e2206856.

[5] a) J. Ackermann, J. T. Metternich, S. Herbertz, S. Kruss, *Angew. Chem. Int. Ed.* **2022**, *61*, e202112372; b) S. Kruss, A. J. Hilmer, J. Zhang, N. F. Reuel, B. Mu, M. S. Strano, *Adv. Drug Deliv. Rev.* **2013**, *65*, 1933; c) H. M. Dewey, A. Lamb, J. Budhathoki-Uprety, *Nanoscale* **2024**, *16*, 16344; d) S. Basu, A. Hendler-Neumark, G. Bisker, *ACS Sens.* **2024**, *9*, 2237; e) M. Yoon, Y. Lee, S. Lee, Y. Cho, D. Koh, S. Shin, C. Tian, Y. Song, J. Kang, S.-Y. Cho, *Sens. Diagn.* **2024**, *3*, 203; f) S. Basu, A. Hendler-Neumark, G. Bisker, *ACS Appl. Mater. Interfaces.* **2024**, *16*, 54960; g) M. Kim, J. J. McCann, J. Fortner, E. Randall, C. Chen, Y. Chen, Z. Yaari, Y. Wang, R. L. Koder, D. A. Heller, *J. Am. Chem. Soc.* **2024**, *146*, 12454; h) M. Kim, C. Chen, Z. Yaari, R. Frederiksen, E. Randall, J. Wollowitz, C. Cupo, X. Wu, J. Shah, D. Worroll et al., *Nat. Chem. Biol.* **2023**, *19*, 1448.

[6] a) L. Wieland, H. Li, C. Rust, J. Chen, B. S. Flavel, *Adv. Energy Mater.* **2021**, *11*; b) L. Dai, D. W. Chang, J.-B. Baek, W. Lu, *Small* **2012**, *8*, 1130.

[7] a) J. Zhang, M. P. Landry, P. W. Barone, J.-H. Kim, S. Lin, Z. W. Ulissi, D. Lin, B. Mu, A. A. Boghossian, A. J. Hilmer et al., *Nat. Nanotechnol.* **2013**, *8*, 959; b) A. J. Gillen, A. A. Boghossian, *Front. chem.* **2019**, *7*, 612; c) A. J. Gillen, J. Kupis-Rozmysłowicz, C. Gigli, N. Schuergers, A. A. Boghossian, *J. Phys. Chem. Lett.* **2018**, *9*, 4336; d) F. A. Mann, N. Herrmann, F. Opazo, S. Kruss, *Angew. Chem. Int. Ed.* **2020**, *59*, 17732; e) A. López-Moreno, J. Villalva, E. M. Pérez, *Chem. Soc. Rev.* **2022**, *51*, 9433; f) J. T. Metternich, J. A. C. Wartmann, L. Sistemich, R. Nißler, S. Herbertz, S. Kruss, *J. Am. Chem. Soc.* **2023**, *145*, 14776; g) M. Kim, C. Chen, P. Wang, J. J. Mulvey, Y. Yang, C. Wun, M. Antman-Passig, H.-B. Luo, S. Cho, K. Long-Roche et al., *Nat. Biomed. Eng.* **2022**, *6*, 267; h) A. Setaro, M. Adeli, M. Glaeske, D. Przyrembel, T. Bisswanger, G. Gordeev, F. Maschietto, A. Faghani, B. Paulus, M. Weinelt et al., *Nat. Commun.* **2017**, *8*, 14281; i) Y. Niidome, R. Hamano, K. Nakamura, S. Qi, S. Ito, B. Yu, Y. Nagai, N. Tanaka, T. Mori, Y. Katayama et al., *Carbon* **2024**, *216*, 118533; j) A. G. Godin, A. Setaro, M. Gandil, R. Haag, M. Adeli, S. Reich, L. Cognet, *Sci. Adv.* **2019**, *5*, eaax1166; k) L. Chio, R. L. Pinals, A. Murali, N. S. Goh, M. P. Landry, *Adv. Funct. Mat.* **2020**, *30*; l) C. F. Chiu, W. A. Saidi, V. E. Kagan, A. Star, *J. Am. Chem. Soc.* **2017**, *139*, 4859; m) H. Kwon, M. Kim, B. Meany, Y. Piao, L. R. Powell, Y. Wang, *J. Phys. Chem. C* **2015**, *119*, 3733; n) T. Shiraki, H. Onitsuka, T. Shiraishi, N. Nakashima, *Chem. Commun.* **2016**, *52*, 12972; o) N. Danné, M. Kim, A. G. Godin, H. Kwon, Z. Gao, X. Wu, N. F. Hartmann, S. K. Doorn, B. Lounis, Y. Wang et al., *ACS nano* **2018**, *12*, 6059; p) Y. Niidome, H. Matsumoto, R. Hamano, K. Kato, T. Fujigaya, T. Shiraki, *J. Phys. Chem. C* **2024**, *128*, 5146.

[8] J. Zaumseil, *Adv. Opt. Mater.* **2022**, *10*.

[9] F. J. Berger, J. Lüttgens, T. Nowack, T. Kutsch, S. Lindenthal, L. Kistner, C. C. Müller, L. M. Bongartz, V. A. Lumsargis, Y. Zakharko et al., *ACS nano* **2019**, *13*, 9259.

[10] A. H. Brozena, M. Kim, L. R. Powell, Y. Wang, *Nat. Rev. Chem.* **2019**, *3*, 375.

[11] H. Kwon, A. Furmanchuk, M. Kim, B. Meany, Y. Guo, G. C. Schatz, Y. Wang, *J. Am. Chem. Soc.* **2016**, *138*, 6878.

[12] C. Ma, C. A. Schrage, J. Gretz, A. Akhtar, L. Sistemich, L. Schnitzler, H. Li, K. Tschulik, B. S. Flavel, S. Kruss, *ACS nano* **2023**, *17*, 15989.

[13] F. L. Sebastian, N. F. Zorn, S. Settele, S. Lindenthal, F. J. Berger, C. Bendel, H. Li, B. S. Flavel, J. Zaumseil, *J. Phys. Chem. Lett.* **2022**, *13*, 3542.

[14] a) N. F. Hartmann, K. A. Velizhanin, E. H. Haroz, M. Kim, X. Ma, Y. Wang, H. Htoon, S. K. Doorn, *ACS nano* **2016**, *10*, 8355; b) M.-K. Li, A. Riaz, M. Wederhake, K. Fink, A. Saha, S. Dehm, X. He, F. Schöppler, M. M. Kappes, H. Htoon et al., *ACS nano* **2022**, *16*, 11742; c) X. He, N. F. Hartmann, X. Ma, Y. Kim, R. Ihly, J. L. Blackburn, W. Gao, J. Kono, Y. Yomogida, A. Hirano et al., *Nat. Photon.* **2017**, *11*, 577; d) Y. Konno, M. Yamada, M. Suzuki, Y. Maeda, *Chemistry* **2023**, *29*, e202301707.

[15] L. Cognet, D. A. Tsyboulski, J.-D. R. Rocha, C. D. Doyle, J. M. Tour, R. B. Weisman, *Science* **2007**, *316*, 1465.

[16] a) D. Kozawa, X. Wu, A. Ishii, J. Fortner, K. Otsuka, R. Xiang, T. Inoue, S. Maruyama, Y. Wang, Y. K. Kato, *Nat. Commun.* **2022**, *13*; b) Y. Piao, B. Meany, L. R. Powell, N. Valley, H. Kwon, G. C. Schatz, Y. Wang, *Nat. Chem.* **2013**, *5*, 840; c) X. Ma, J. K. S. Baldwin, N. F. Hartmann, S. K. Doorn, H. Htoon, *Adv. Funct. Mat.* **2015**, *25*, 6157; d) D. Janas, *Mater. Horiz.* **2020**, *7*, 2860; e) T. Shiraki, Y. Miyauchi, K. Matsuda, N. Nakashima, *Acc. Chem. Res.* **2020**, *53*, 1846.

[17] a) A. D. McNaught, A. Wilkinson, *IUPAC, Compendium of Chemical Terminology, The "Gold book"*, Blackwell Scientific Publications, Oxford, **1997**; b) T. Friščić, C. Mottillo, H. M. Titi, *Angew. Chem. Int. Ed.* **2020**, *59*, 1018; c) S. L. James, C. J. Adams, C. Bolm, D. Braga, P. Collier, T. Friščić, F. Grepioni, K. D. M. Harris, G. Hyett, W. Jones et al., *Chem. Soc. Rev.* **2012**, *41*, 413; d) L. Dong, L. Li, H. Chen, Y. Cao, H. Lei, *Adv. Sci.* **2024**, e2403949.

[18] a) M. Sander, S. Fabig, L. Borchardt, *Chem. Eur. J.* **2023**, *29*, e202202860; b) K. J. Ardila-Fierro, J. G. Hernández, *ChemSusChem* **2021**, *14*, 2145; c) J. Andersen, J. Mack, *Green Chem.* **2018**, *20*, 1435; d) S. Ni, M. Hribersek, S. K. Baddigam, F. J. L. Ingner, A. Orthaber, P. J. Gates, L. T. Pilarski, *Angew. Chem. Int. Ed.* **2021**, *60*, 6660; e) F. Cuccu, L. de Luca, F. Delogu, E. Colacino, N. Solin, R. Mocci, A. Porcheddu, *ChemSusChem* **2022**, *15*, e202200362.

[19] L. Gonnet, C. B. Lennox, J.-L. Do, I. Malvestiti, S. G. Koenig, K. Nagapudi, T. Friščić, *Angew. Chem. Int. Ed.* **2022**, *61*, e202115030.

[20] a) S.-E. Zhu, F. Li, G.-W. Wang, *Chem. Soc. Rev.* **2013**, *42*, 7535; b) N. Rubio, C. Fabbro, M. A. Herrero, A. de La Hoz, M. Meneghetti, J. L. G. Fierro, M. Prato, E. Vázquez, *Small* **2011**, *7*, 665; c) K. Ptaszyńska, A. Malaika, K. Morawa Eblagon, J. L. Figueiredo, M. Kozłowski, *Molecules* **2024**, *29*; d) H. Pan, L. Liu, Z.-X. Guo, L. Dai, F. Zhang, D. Zhu, R. Czerw, D. L. Carroll, *Nano Lett.* **2003**, *3*, 29.

[21] a) D. Leistenschneider, K. Zürbes, C. Schneidermann, S. Grätz, S. Oswald, K. Wegner, B. Klemmed, L. Giebeler, A. Eychmüller, L. Borchardt, *C* **2018**, *4*, 14; b) N. Welham, V. Berbenni, P. Chapman, *Carbon* **2002**, *40*, 2307; c) M. Pandurangappa, T. Ramakrishnappa, R. G. Compton, *Carbon* **2009**, *47*, 2186.

[22] a) H. Harker, J. B. Horsley, D. Robson, *Carbon* **1971**, *9*, 1; b) V. León, M. Quintana, M. A. Herrero, J. L. G. Fierro, A. de La Hoz, M. Prato, E. Vázquez, *Chem. Commun.* **2011**, *47*, 10936; c) N. C. Deb Nath, I.-Y. Jeon, M. J. Ju, S. A. Ansari, J.-B. Baek, J.-J. Lee, *Carbon* **2019**, *142*, 89; d) M.-J. Kim, I.-Y. Jeon, J.-M. Seo, L. Dai, J.-B. Baek, *ACS nano* **2014**, *8*, 2820.

[23] a) D. F. Chowdhury, Z. F. Cui, *Carbon* **2011**, *49*, 862; b) N. Pierard, A. Fonseca, J.-F. Colomer, C. Bossuot, J.-M. Benoit, G. van Tendeloo, J.-P. Pirard, J. Nagy, *Carbon* **2004**, *42*, 1691; c) J.-H. Ahn, H.-S. Shin, Y.-J. Kim, H. Chung, *J. Alloys Compd.* **2007**, *434-435*, 428; d) Z. Kónya, I.

5

Vesselenyi, K. Niesz, A. Kukovecz, A. Demortier, A. Fonseca, J. Delhalle, Z. Mekhalif, J. B.Nagy, A. A. Koós et al., *Chem. Phys. Lett.* **2002**, *360*, 429; e) Á. Kukovecz, T. Kanyó, Z. Kónya, I. Kiricsi, *Carbon* **2005**, *43*, 994.

[24]   a) X. Li, J. Shi, Y. Qin, Q. Wang, H. Luo, P. Zhang, Z.-X. Guo, H.-S. Woo, D.-K. Park, *Chem. Phys. Lett.* **2007**, *444*, 258; b) P. C. Ma, S. Q. Wang, J.-K. Kim, B. Z. Tang, *J. Nanosci. Nanotechnol.* **2009**, *9*, 749; c) R. Barthos, D. Méhn, A. Demortier, N. Pierard, Y. Morciaux, G. Demortier, A. Fonseca, J. B. Nagy, *Carbon* **2005**, *43*, 321; d) C. A. Dyke, J. M. Tour, *J. Am. Chem. Soc.* **2003**, *125*, 1156; e) B. K. Price, J. L. Hudson, J. M. Tour, *J. Am. Chem. Soc.* **2005**, *127*, 14867; f) M. Holzinger, O. Vostrowsky, A. Hirsch, F. Hennrich, M. Kappes, R. Weiss, F. Jellen, *Angew. Chem. Int. Ed.* **2001**, *40*, 4002; g) M. Holzinger, J. Abraham, P. Whelan, R. Graupner, L. Ley, F. Hennrich, M. Kappes, A. Hirsch, *J. Am. Chem. Soc.* **2003**, *125*, 8566.

[25]   A. Stolle, R. Schmidt, K. Jacob, *Faraday Discuss.* **2014**, *170*, 267.

[26]   a) H. Shin, S. Lee, H. Suk Jung, J.-B. Kim, *Ceram. Int.* **2013**, *39*, 8963; b) A. Stolle, B. Ranu, *Ball Milling Towards Green Synthesis*, Royal Society of Chemistry, Cambridge, **2014**.

[27]   O. F. Jafter, S. Lee, J. Park, C. Cabanetos, D. Lungerich, *Angew. Chem. Int. Ed.* **2024**, e202409731.

[28]   a) C. Burmeister, L. Titscher, S. Breitung-Faes, A. Kwade, *Adv. Powder Technol.* **2018**, *29*, 191; b) C. F. Burmeister, M. Hofer, P. Molaiyan, P. Michalowski, A. Kwade, *Processes* **2022**, *10*, 692.

[29]   a) J.-L. Do, T. Friščić, *Synlett* **2017**, *28*, 2066; b) T. Friščić, S. L. Childs, S. A. A. Rizvi, W. Jones, *CrystEngComm* **2009**, *11*, 418.

[30]   L. Gonnet, T. H. Borchers, C. B. Lennox, J. Vainauskas, Y. Teoh, H. M. Titi, C. J. Barrett, S. G. Koenig, K. Nagapudi, T. Friščić, *Faraday Discuss.* **2023**, *241*, 128.

[31]   a) M. Wohlgemuth, S. Schmidt, M. Mayer, W. Pickhardt, S. Grätz, L. Borchardt, *Chem. Eur. J.* **2023**, *29*, e202301714; b) R. Tanaka, N. Takahashi, Y. Nakamura, Y. Hattori, K. Ashizawa, M. Otsuka, *RSC Adv.* **2016**, *6*, 87049.

[32]   a) J. T. Metternich, B. Hill, J. A. C. Wartmann, C. Ma, R. M. Kruskop, K. Neutsch, S. Herbertz, S. Kruss, *Angew. Chem. Int. Ed.* **2024**, *63*, e202316965; b) F. A. Mann, P. Galonska, N. Herrmann, S. Kruss, *Nat. Protoc.* **2022**, *17*, 727.

6

Entry for the Table of Contents
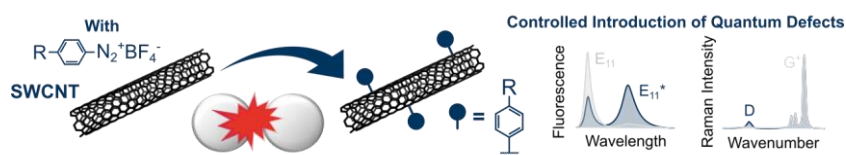
Tailoring the photophysics of single-walled carbon nanotubes (SWCNTs) holds immense potential for their applications in sensing and imaging. By using mechanochemistry, sp^3 quantum defects are introduced in fluorescent SWCNTs via a solid-state reaction within 5 min. This method allows by varying the mechanochemical energy impact to create quantum defects at extremely low defect densities and chemical control without diminishing fluorescence.

Institute and/or researcher Twitter usernames: @Borchardt_Group